Chapter 19

Attitude Determination

Clark E. Cohen*
Stanford University, Stanford, California 94305

ALTHOUGH originally developed as a means for navigation, GPS has since been shown to be an abundant source of attitude information as well. Using the subcentimeter precision of GPS carrier phase, a receiver can determine the relative positions of multiple antennas mounted to vehicles or platforms so accurately that their orientation may be determined in real time at output rates exceeding 10 Hz. This chapter discusses the fundamentals of attitude determination using GPS. It also describes the mathematics of attitude solution processing, error evaluation, and cycle ambiguity resolution. Finally, it discusses applications and provides a sample of experimental results.

I. Overview

The fundamental principle of attitude determination with GPS and multiple antennas is shown in Fig. 1. The GPS satellite is so distant relative to the antenna separation that arriving wavefronts can be considered as effectively planar. A signal traveling at the speed of light arrives at the antenna closer to the satellite slightly before reaching the other. By measuring the difference in carrier phase between the antennas, a receiver can determine the relative range between the pair of antennas. With the addition of carrier phase measurements from multiple satellites using three or more antennas, the receiver can estimate the full three-axis attitude of an object.

Early experimental work employed TRANSIT satellites for attitude determination.[1] Since then, many GPS receivers have been developed or adapted for carrying out attitude determination. Examples of these include implementations by Magnavox,[2] Trimble,[3] TI, [4] and Ashtech.[5]

In the conventional relative position fix (for example, between two survey receivers), range difference measurements between the two receivers from *four* GPS satellites are required to solve for the three components of Cartesian relative position and receiver clock time bias. For attitude determination, it is possible

*Research Associate, Department of Aeronautics and Astronautics; Manager of GPS Precision Landing.

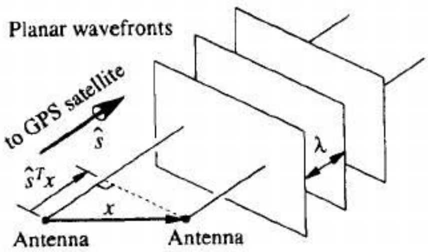

Fig. 1 Attitude geometry.

to configure the receiver so that *only two GPS satellites in view are explicitly required.* There are two reasons for this.

1) *Common Time Reference:* If the receiver is designed as shown in Fig. 2, so that each signal path shares a common time reference, the phase difference measurement precision is maximized. Because any local oscillator variations affect both signal paths identically, these variations cancel out in the final differencing process. Therefore, the measurements are *independent* of the receiver clock bias. Because of the electrical connection between antennas, only signals from *three* GPS satellites are required to find the three Cartesian components of relative antenna position.

2) *Fixed Baseline Configuration:* For attitude determination, the relative mechanical placement of the antennas must be known in advance. Given the additional rigid constraint on relative antenna placement on the vehicle, another satellite measurement can be dropped. Therefore, a minimum of only *two* GPS satellites are required for an attitude fix.

This result provides some very practical benefits. First, overall solution integrity is improved considerably. Because the operational GPS constellation provides at least four satellites in view, attitude solutions are, in general, strongly overdetermined. Occasional cycle slips can be detected and isolated in real time. Second, when the vehicle attitude tips to extremes (such as with an aircraft in a steep angle of bank), attitude solutions are uninterrupted as long as at least two satellites are in view.

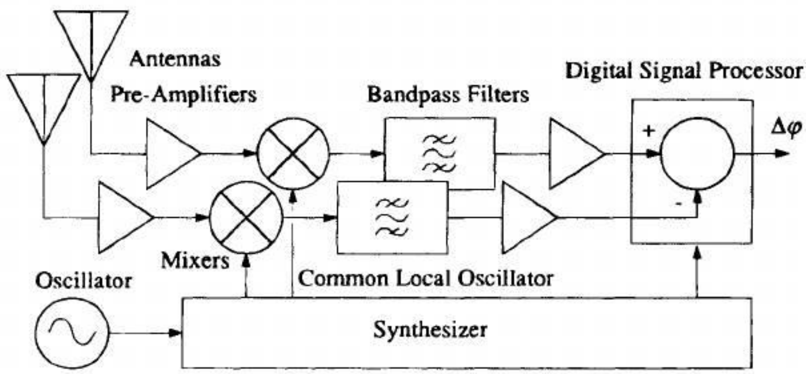

Fig. 2 Common local oscillator.

Referring to Fig. 3, the measured differential phase, $\Delta\varphi$ (measured in wavelengths), is proportional to the projection (vector dot product) of the baseline vector $\boldsymbol{x}$ (3×1), measured in wavelengths (cycles), into the line of sight unit vector to the satellite, $\hat{\boldsymbol{s}}$ (3×1), for baseline i and satellite j. However, as implied in the figure the GPS receiver initially only measures the fractional part of the differential phase. The integer component k must be resolved through independent means before the differential phase measurement can be interpreted as a differential range measurement. The resulting expression is then $\Delta\varphi_{ij} = \hat{\boldsymbol{s}}_j^T \boldsymbol{x}_i - k_{ij} + v_{ij}$, where v_{ij} is additive, time-correlated measurement noise from the relative ranging error sources discussed in Sec. V. Note that in this chapter as a matter of convention, the integer k_{ij} is treated as a *constant* as long as continuous lock is maintained (i.e., until a cycle slip occurs) on that combination of satellite and baseline. In other words, the initial allocation of integer component between k and $\Delta\varphi$ is *arbitrary*. As the satellite–baseline geometry changes with time, it is assumed that the *receiver tracking loops keep automatic track of integer wrap-arounds* in the $\Delta\varphi$ measurements as they occur (i.e., they track the total change in $\Delta\varphi$, including the integer part). Thus, the only ambiguity is the initial value of the integer k. Also note that the line bias attributable to electrical path length differences is not treated in this expression or those which follow, because it can generally be removed through receiver calibration.

II. Fundamental Conventions for Attitude Determination

Although a full discussion of the mathematical tools generally used for attitude determination is beyond the scope of this book, some introductory material on the fundamental conventions for attitude determination is supplied here as a minimum basis for understanding coordinate transformations and attitude parameterization. For a more in-depth description of these concepts, see Ref. 6.

In attitude determination, we typically are concerned with describing a vehicle system in two separate reference frames: the local horizontal (or, alternatively,

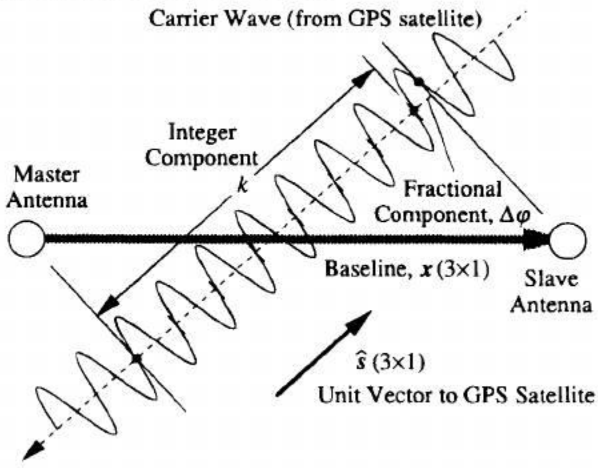

Fig. 3 Observation geometry.

an inertial) coordinate system and the vehicle body coordinate system. As shown in Fig. 4, the vehicle body coordinate axes (dashed; designated as unit vectors $\boldsymbol{x}'$, $\boldsymbol{y}'$, and $\boldsymbol{z}'$) are generally rotated with respect to the local horizontal coordinate frame axes (solid; designated as unit vectors $\boldsymbol{x}$, $\boldsymbol{y}$, and $\boldsymbol{z}$). Each coordinate frame is right-handed (i.e., $\boldsymbol{x}$ crossed into $\boldsymbol{y}$ equals $\boldsymbol{z}$). A given vector $\boldsymbol{r}$ (3×1) is expressed in the local horizontal coordinate frame. The same vector $\boldsymbol{r}$ can also be expressed as $\boldsymbol{r}'$ in the vehicle body (primed) reference frame through a *coordinate transformation:* $\boldsymbol{r}' = A\boldsymbol{r}$.

The matrix A (3×3) is known as the *attitude matrix* or *direction cosine matrix.* The easiest way to construct the attitude matrix is by assembling the dot products of the orthogonal coordinate frame unit vectors:

$$A = \begin{bmatrix} \boldsymbol{x}' \cdot \boldsymbol{x} & \boldsymbol{x}' \cdot \boldsymbol{y} & \boldsymbol{x}' \cdot \boldsymbol{z} \\ \boldsymbol{y}' \cdot \boldsymbol{x} & \boldsymbol{y}' \cdot \boldsymbol{y} & \boldsymbol{y}' \cdot \boldsymbol{z} \\ \boldsymbol{z}' \cdot \boldsymbol{x} & \boldsymbol{z}' \cdot \boldsymbol{y} & \boldsymbol{z}' \cdot \boldsymbol{z} \end{bmatrix}$$

Although there are nine elements in the matrix, they are not all independent. There are really only three DOF because of the orthonormal constraints ($A^TA = I$) placed on the transformation. The inverse of any attitude matrix is simply its transpose.

The most commonly accepted convention for defining coordinate frames and rotation angles is shown in Fig. 5. Rotations are defined in a specific Euler sequence about the coordinate axes. The axes of the local horizontal frame are such that the $\boldsymbol{x}$ axis points due north, the $\boldsymbol{y}$ axis points due east, and the $\boldsymbol{z}$ axis points directly downward along the local vertical to complete the right-handed set of axes. The body reference frame is fixed to the aircraft so that the $\boldsymbol{x}'$ (roll) axis points out the nose, the $\boldsymbol{y}'$ axis points to the right along the wing, and the $\boldsymbol{z}'$ axis points out the belly to complete the right-handed coordinate axis set. The figure shows the body frame when the pitch and roll angles are zero. For this special case, the pitch axis is aligned with the $\boldsymbol{y}'$ axis, and the heading axis is aligned with the $\boldsymbol{z}'$ axis (local vertical). When the heading, pitch, and roll angles are all zero, the body frame is aligned with the local horizontal frame ($A = I$).

Given this introduction, the three attitude angles (heading, pitch, and roll) may then specify the vehicle attitude. Starting from the reference attitude (where

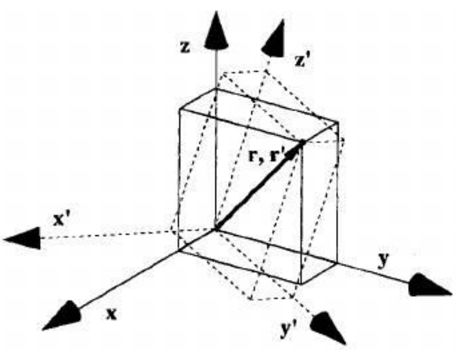

Fig. 4 Coordinate transformation.

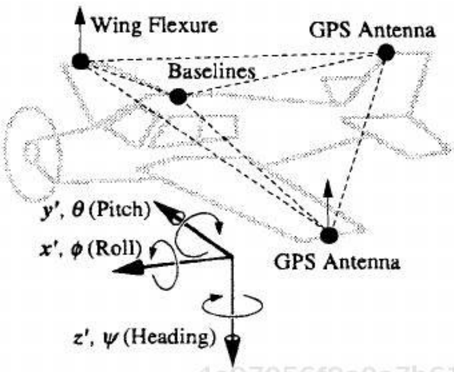

Fig. 5 Aircraft geometry.

the body and local horizontal coordinate frames are aligned), the body frame is rotated (always in a positive, right-handed sense) about the local vertical downward z axis by the heading angle ψ. Then, the body frame is rotated about the new pitch axis by the pitch angle θ. Finally, the body frame is rotated about the roll x' axis by the roll angle ϕ. The resulting attitude matrix A can be shown to be as follows:

$$A = \begin{bmatrix} \cos\theta\cos\psi & \cos\theta\sin\psi & -\sin\theta \\ -\cos\phi\sin\psi + \sin\phi\sin\theta\cos\psi & \cos\phi\cos\psi + \sin\phi\sin\theta\sin\psi & \sin\phi\cos\theta \\ \sin\phi\sin\psi + \cos\phi\sin\theta\cos\psi & -\sin\phi\cos\psi + \cos\phi\sin\theta\sin\psi & \cos\phi\cos\theta \end{bmatrix}$$

III. Solution Processing

This section discusses how differential phase measurements can be converted into attitude solutions. To clarify presentation, it is first assumed that the cycle ambiguities are already known. Discussion of the processes for resolving integers is deferred until Sec. IV. If the integers are known, then the differential *phase* measurements can be treated explicitly as differential *range* measurements through the relationship $\Delta r = \Delta\varphi + k$. Then the process of attitude determination consists of converting these differential range measurements into attitude solutions. An optimal attitude solution for a given set of range measurements Δr_{ij} taken at a single epoch for baseline i and satellite j is obtained by minimizing the quadratic attitude determination cost function:

$$J(A) = \sum_{i=1}^{m} \sum_{j=1}^{n} (\Delta r_{ij} - b_i^T A \hat{s}_j)^2$$

for the m baseline and n satellites, where $\boldsymbol{b}$ (3×1) is the baseline vector defined in the body frame, $\hat{\boldsymbol{s}}$ (3×1) is the line of sight to the GPS satellite given in the local horizontal frame, and A (3×3), the variable to be used in minimization, is the right-handed, orthonormal attitude transformation ($\det A = 1$, $A^T A = I$) from the local horizontal frame to the body frame.

Given a trial attitude matrix A_0, a better estimate may be obtained by linearizing this cost function about the trial solution and solving for a correction matrix δA.

Solving for the best correction matrix during iteration p yields a new and better trial matrix for iteration $p + 1$, so that $A_{p+1} = \delta A_p A_p$. A simple correction matrix can be constructed of small-angle rotations, so that $\delta A(\boldsymbol{\delta\theta}) \cong I + \Theta^{\times}$, where I (3 × 3) is the identity matrix, and $\boldsymbol{\delta\theta}$ (3 × 1) is a vector of small-angle rotations about the following three body frame axes:

$$\boldsymbol{\delta\theta} = \begin{bmatrix} \delta\theta_{x'} \\ \delta\theta_{y'} \\ \delta\theta_{z'} \end{bmatrix}$$

and $\Theta^{\times}$ (3 × 3) is the skew-symmetric matrix associated with the vector $\boldsymbol{\delta\theta}$.

$$\Theta^{\times} = \begin{bmatrix} 0 & -\delta\theta_{z'} & \delta\theta_{y'} \\ \delta\theta_{z'} & 0 & -\delta\theta_{x'} \\ -\delta\theta_{y'} & \delta\theta_{x'} & 0 \end{bmatrix}$$

so that $\Theta^{\times}\boldsymbol{b} = \boldsymbol{\delta\theta} \times \boldsymbol{b}$. The attitude cost function becomes the following:

$$J(\boldsymbol{\delta\theta})\,|_{A_0} \cong \sum_{i=1}^{m}\sum_{j=1}^{n} [\Delta r_{ij} - \boldsymbol{b}_i^T(I + \Theta^{\times})A_0\hat{\boldsymbol{s}}_j]^2 = \sum_{i=1}^{m}\sum_{j=1}^{n} (\delta r_{ij} - \boldsymbol{b}_i^T\Theta^{\times}A_0\hat{\boldsymbol{s}}_j)^2$$

where $\delta r_{ij} \equiv \Delta r_{ij} - \boldsymbol{b}_i^T A_0 \hat{\boldsymbol{s}}_j$. The measurement geometry is described by the rightmost term, which may be rewritten directly in terms of the three attitude correction angles about each axis $\boldsymbol{b}_i^T\Theta^{\times}A_0\hat{\boldsymbol{s}}_j = \hat{\boldsymbol{s}}_j^T A_0^T \Theta^{\times}\boldsymbol{b}_i = \hat{\boldsymbol{s}}_j^T A_0^T B_i^{\times}\boldsymbol{\delta\theta}$.

Because the right-hand side of this result can also be written as

$$[(A_0\hat{\boldsymbol{s}}_j) \times \boldsymbol{b}_i] \cdot \boldsymbol{\delta\theta},$$

the implication is that the attitude angle sensitivity to a measurement from a given baseline and GPS satellite is simply the *cross-product* of the line-of-sight vector with the baseline vector. The linearized cost function may now be written as follows:

$$\delta J(\boldsymbol{\delta\theta})\,|_{A_0} = \| H\boldsymbol{\delta\theta} - \boldsymbol{\delta r} \|_2^2$$

where $\boldsymbol{\delta r}$ is the vector formed by stacking all measurements, and H is the observation matrix formed by stacking the measurement geometry for each separate measurement:

$$H = \begin{bmatrix} \vdots \\ \hat{\boldsymbol{s}}_j^T A_0^T B_i^{\times} \\ \vdots \end{bmatrix}$$

The estimate for A is then refined iteratively until the process converges to the numerical precision of the computer.

In cases where the baseline array is non–co-planar, there is an algorithm for carrying out the attitude calculation approximately an order of magnitude faster. This approach is based on solving "Wahba's Problem" of attitude determination using vector observations.[7]

IV. Cycle Ambiguity Resolution

As suggested in Fig. 3, cycle ambiguity resolution is the process of determining the integer number of wavelengths that lie between a given pair of antennas along a particular line of sight. It is the key initialization step that must be performed before attitude determination using GPS can commence.

A. Baseline Length Constraint

Consider a platform with a single baseline constructed from two antennas. The baseline vector originates at the master antenna and ends at the slave antenna. Because differential positioning is employed, no generality is sacrificed by assuming that the tail of the vector stays fixed in space, as shown in Fig. 6. The possible positions of the slave antenna are constrained to lie on the surface of a virtual sphere of radius equal to the baseline length.

B. Integer Searches

The most brute force method of resolving the integers is the search method. In an integer search, all possible combinations of candidate integers (which can number in the hundreds of millions for antenna separations of even just a few meters) are systematically checked against a cost function until (it is hoped) the correct set is found.

Although search techniques work accurately and quickly for smaller baselines (on the order of several carrier wavelengths), they are vulnerable to erroneous solutions with longer baselines or when few satellites are visible. Although many creative techniques have been synthesized for maximizing the execution speed of the search process,[8–10] searches still occasionally suffer from ambiguous results.

The search technique is depicted to scale in Fig. 7 for a single 4λ baseline, three satellites, and 3σ multipath error. The instantaneous satellite line-of-sight vectors are depicted with arrows. Possible integer values are shown as concentric bands about the line-of-sight vectors. The correct integer set is indicated in white. Any place on the sphere where the concentric bands for all three satellites intersect (indicated in black) is a viable baseline orientation candidate. *Note that at any one instant, there is not a unique solution.*

C. Motion-Based Methods

Although lacking the near-instantaneous start-up time of integer search methods, motion-based methods are unmatched for providing the highest level of

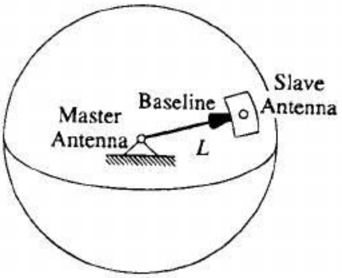

Fig. 6 Length constraint.

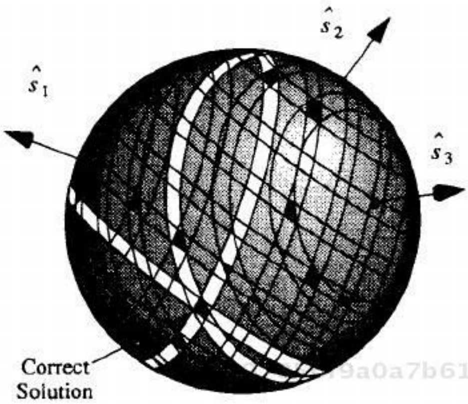

Fig. 7 Integer search.

overall solution integrity.[11] Motion-based integer resolution algorithms make use of the abundance of information provided by platform or GPS satellite motion. This attitude motion modulates the relative carrier phase with a signature that may be used to identify the cycle ambiguities. If the motion occurs rapidly enough, this process is complete within seconds. Rather than constraining cycle ambiguities to lie on integer values, motion-based methods estimate the cycle ambiguities as continuous biases. Checking without imposing the integer constraint that the bias values indeed lie near integer values provides a unique, unambiguous solution with extraordinary integrity—even when there are only a few satellites in view.

For aircraft applications, natural attitude motion consists of banks, turns, or attitude perturbations excited by turbulence. If the baseline vectors are non–coplanar, even a turn on the ground (about a single axis) is sufficient for cycle ambiguity resolution.

Without knowledge of the integers, it is possible to determine the Cartesian position of the slave antenna relative to its unknown starting point. The differential phase measurement equation may be expressed in compact vector and matrix notation for the n satellites in view (neglecting ranging noise):

$$\boldsymbol{\Delta\varphi} = S^T\boldsymbol{x} - \boldsymbol{k}$$

where

$$\boldsymbol{\Delta\varphi}(n \times 1) = \begin{bmatrix} \Delta\varphi_1 \\ \Delta\varphi_2 \\ \vdots \\ \Delta\varphi_n \end{bmatrix}, \qquad S(3 \times n) = [\hat{\boldsymbol{s}}_1 \quad \hat{\boldsymbol{s}}_2 \quad \cdots \quad \hat{\boldsymbol{s}}_n],\ \boldsymbol{k}(n \times 1) = \begin{bmatrix} k_1 \\ k_2 \\ \vdots \\ k_n \end{bmatrix}$$

Suppose a baseline moves from Cartesian position $\boldsymbol{x}^{(0)}$ to $\boldsymbol{x}^{(1)}$. The measured change in differential range is given by $\boldsymbol{\Delta\varphi}^{(1)} - \boldsymbol{\Delta\varphi}^{(0)} = S^T[\boldsymbol{x}^{(1)} - \boldsymbol{x}^{(0)}] = S^T\boldsymbol{\Delta x}$. Because the integer ambiguity $\boldsymbol{k}$ cancels out of the above expression, and the satellite line-of-sight vectors are known, we can solve for the displacement vector

Δx (3 × 1), explicitly using a linear least-squares fit. For the integer resolution processing $n = 3$ satellites are used to determine the relative location of the slave antenna undergoing motion. (After cycle resolution is complete, two satellites are required for attitude determination.) It has been assumed that the position displacement is occurring on a much faster time scale than that of the satellite line-of-sight vectors $\hat{s}$.

As baseline motion is occurring, it is possible to accumulate a set of displacement vectors over a short interval of time. If the platform moves by a large angle, the set of displacement vectors can be used to calculate an initial guess to initialize a nonlinear least-squares fit.[4]

A two-dimensional representation of the rigid body antenna mounting constraints is shown in Fig. 8. Suppose that the baseline vector x rotates in space. Here the baseline vector is moved (displaced) by the vector Δx to two different locations at two different times, 1 and 2. If a line is constructed perpendicular to each Δx displacement vector passing through its midpoint, the center of the circle must be included on that line. By simultaneously considering each Δx vector, the center of the circle can be located, along with the initial position x of the baseline.

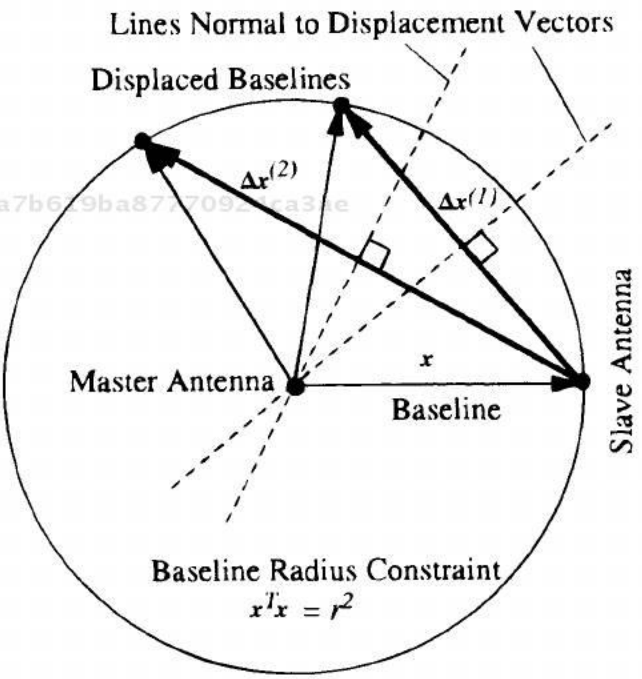

Fig. 8 Large angle motion: initial guess

Mathematically, the solution may be developed by constructing the square of the norm of the rotated baseline vector $\boldsymbol{x} + \boldsymbol{\Delta x}$, given as follows:

$$(\boldsymbol{x} + \boldsymbol{\Delta x})^T(\boldsymbol{x} + \boldsymbol{\Delta x}) = \boldsymbol{x}^T\boldsymbol{x} + 2\boldsymbol{\Delta x}^T\boldsymbol{x} + \boldsymbol{\Delta x}^T\boldsymbol{\Delta x}$$

Noting that the left side is equal to the square of the baseline length, as is $\boldsymbol{x}^T\boldsymbol{x}$, the two terms may be canceled, leaving $2\boldsymbol{\Delta x}^T\boldsymbol{x} = -\boldsymbol{\Delta x}^T\boldsymbol{\Delta x}$.

Different $\boldsymbol{\Delta x}$ vectors taken at N different times (indicated by a superscript in parentheses) may be stacked into matrix form as follows:

$$2\begin{bmatrix} \boldsymbol{\Delta x}^{(1)T} \\ \boldsymbol{\Delta x}^{(2)T} \\ \vdots \\ \boldsymbol{\Delta x}^{(N)T} \end{bmatrix} \boldsymbol{x} = -\begin{bmatrix} \boldsymbol{\Delta x}^{(1)T}\boldsymbol{\Delta x}^{(1)} \\ \boldsymbol{\Delta x}^{(2)T}\boldsymbol{\Delta x}^{(2)} \\ \vdots \\ \boldsymbol{\Delta x}^{(N)T}\boldsymbol{\Delta x}^{(N)} \end{bmatrix}$$

Then the baseline solution x may be obtained through a linear least-squares fit. Each $\boldsymbol{\Delta x}$ vector defines a subspace in which the slave antenna must lie. The baseline is then the point that comes closest to this condition in a least-squares sense. A convenient shorthand notation for this least-squares fit is given by $2\boldsymbol{\Delta X}^T\boldsymbol{x} = -\mathrm{diag}\left(\boldsymbol{\Delta X}^T\boldsymbol{\Delta X}\right)$, $\boldsymbol{\Delta X}$ $(3 \times N) \equiv [\boldsymbol{\Delta x}^{(1)} \quad \boldsymbol{\Delta x}^{(2)} \quad \cdots \quad \boldsymbol{\Delta x}^{(N)}]$ and diag(•) defines a vector $(N \times 1)$ comprised of the diagonal elements of the argument matrix $(N \times N)$.

Unfortunately, for the single baseline case, large-angle rotation about the two axes perpendicular to the baseline is always required to resolve completely the integer ambiguities using motion. To avoid the shortcoming of requiring two-axis motion perpendicular to each baseline, information from multiple baselines can be combined into a single simultaneous estimation equation.[12] The constraint equation between different baselines i and j yields $\left(\boldsymbol{x}_i + \boldsymbol{\Delta x}_i\right)^T\left(\boldsymbol{x}_j + \boldsymbol{\Delta x}_j\right) = \boldsymbol{x}_i^T\boldsymbol{x}_j + \boldsymbol{x}_i^T\boldsymbol{\Delta x}_j + \boldsymbol{\Delta x}_i^T\boldsymbol{x}_j + \boldsymbol{\Delta x}_i^T\boldsymbol{\Delta x}_j$.

Again, the dot product of each baseline pair is constant; hence, the corresponding term may be canceled from both sides of the equation, leaving $\boldsymbol{\Delta x}_j^T\boldsymbol{x}_i + \boldsymbol{\Delta x}_i^T\boldsymbol{x}_j = -\boldsymbol{\Delta x}_i^T\boldsymbol{\Delta x}_j$.

Combining $\boldsymbol{\Delta x}$ measurements from N different times (typically 10–30 epochs), this form may be expanded as follows:

$$\begin{bmatrix} \boldsymbol{\Delta x}_j^{(1)T} \\ \boldsymbol{\Delta x}_j^{(2)T} \\ \vdots \\ \boldsymbol{\Delta x}_j^{(N)T} \end{bmatrix} \boldsymbol{x}_i + \begin{bmatrix} \boldsymbol{\Delta x}_i^{(1)T} \\ \boldsymbol{\Delta x}_i^{(2)T} \\ \vdots \\ \boldsymbol{\Delta x}_i^{(N)T} \end{bmatrix} \boldsymbol{x}_j = -\begin{bmatrix} \boldsymbol{\Delta x}_i^{(1)T}\boldsymbol{\Delta x}_j^{(1)} \\ \boldsymbol{\Delta x}_i^{(2)T}\boldsymbol{\Delta x}_j^{(2)} \\ \vdots \\ \boldsymbol{\Delta x}_i^{(N)T}\boldsymbol{\Delta x}_j^{(N)} \end{bmatrix}$$

Invoking the same matrix notation as above, the entire initial guess for the case of the three baselines shown in Fig. 9 can be combined into a single, unified least-squares fit equation:

$$\begin{bmatrix} \Delta X_2^T & \Delta X_1^T & 0 \\ \Delta X_3^T & 0 & \Delta X_1^T \\ 0 & \Delta X_3^T & \Delta X_2^T \\ 2\Delta X_1^T & 0 & 0 \\ 0 & 2\Delta X_2^T & 0 \\ 0 & 0 & 2\Delta X_3^T \end{bmatrix} \begin{bmatrix} x_1 \\ x_2 \\ x_3 \end{bmatrix} = - \begin{bmatrix} \mathrm{diag}(\Delta X_1^T \Delta X_2) \\ \mathrm{diag}(\Delta X_1^T \Delta X_3) \\ \mathrm{diag}(\Delta X_3^T \Delta X_2) \\ \mathrm{diag}(\Delta X_1^T \Delta X_1) \\ \mathrm{diag}(\Delta X_2^T \Delta X_2) \\ \mathrm{diag}(\Delta X_3^T \Delta X_3) \end{bmatrix}$$

The left-hand matrix is now $6N \times 9$, the solution vector is 9×1, and the right-hand vector is $6N \times 1$. This same matrix structure applies to any number of baselines. For the case of three or more baselines, two important advantages fall out of this approach.

First, with motion about any two *arbitrary* axes, no a priori information about antenna placement is required to unambiguously solve for all three of the three initial baseline vectors (three components each, nine total dimensions). It is the measurements themselves that are providing all the geometrical information. Therefore, this approach could be adapted to perform *in situ* self-calibration of GPS baselines during normal operation.

Second, by incorporating the known baseline constraints in the case of non–coplanar baseline configurations, *motion about a single axis of rotation is entirely adequate for an unambiguous baseline vector solution.*

1. *Measurement Refinement*

To refine the initial guess iteratively, a new cost function (modeled after the one defined in Sec. III) is employed:

$$J(A^{(1)}, A^{(2)}, \ldots, A^{(N)}, \boldsymbol{k}) = \sum_{\ell=1}^{N} \sum_{i=1}^{m} \sum_{j=1}^{n} (\Delta\varphi_{ij}^{(\ell)} + \boldsymbol{k}_{ij} - \boldsymbol{b}_i^T A^{(\ell)} \boldsymbol{s}_j^{(\ell)})^2$$

where $A^{(\ell)}$ is the attitude matrix at each epoch ℓ, and $\boldsymbol{k}$ is a vector of the cycle ambiguities for all the baseline and antenna combinations. The ambiguities are estimated as continuous variables.

The problem is to find the independent attitude matrices at each epoch and the set of integers (which applies to all epochs) that minimize the stated cost function. For each epoch, it is possible to convert the initial guess of baseline position given above into an initial guess for the attitude A_0. As shown in Sec. III, the cost function can then be linearized about this initial guess. The attitude component of the state variables to be estimated consists of perturbations in the vehicle attitude about all three axes for every epoch l under consideration. The

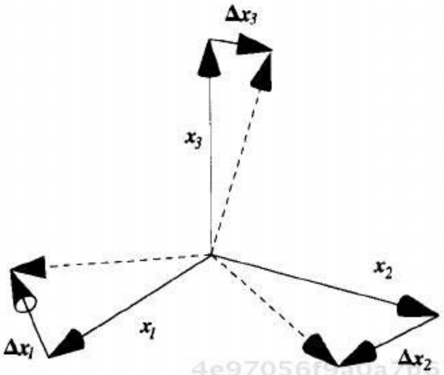

Fig. 9 Non–co-planar baseline rotation.

resulting linearized equations are as follows:

$$\left[\begin{array}{cccc|c} H_1 & 0 & 0 & 0 & -I \\ 0 & H_2 & & 0 & -I \\ \vdots & & \ddots & \vdots & \vdots \\ 0 & 0 & \cdots & H_N & -I \end{array}\right]\left[\begin{array}{c} \boldsymbol{\delta\theta}^{(1)} \\ \boldsymbol{\delta\theta}^{(2)} \\ \vdots \\ \boldsymbol{\delta\theta}^{(N)} \\ \hline \boldsymbol{k} \end{array}\right] = \begin{bmatrix} \boldsymbol{\delta\varphi}^{(1)} \\ \boldsymbol{\delta\varphi}^{(2)} \\ \vdots \\ \boldsymbol{\delta\varphi}^{(N)} \end{bmatrix}$$

where each $H_l(mn \times 3)$ is the sensitivity matrix of changes in measured differential phase with respect to rotations about each of the three axes of attitude, and I $(mn \times mn)$ is the identity matrix. As was shown in Sec. III, each row of H is given by $(A_0^{(l)} S_j^{(l)}) \times \boldsymbol{b}_i$. The other state variables are as follows:

$$\boldsymbol{\delta\theta}^{(\ell)}(3 \times 1) = \begin{bmatrix} \delta\theta_x^{(\ell)} \\ \delta\theta_y^{(\ell)} \\ \delta\theta_z^{(\ell)} \end{bmatrix} \quad \text{and} \quad \boldsymbol{k}(mn \times 1) = \begin{bmatrix} k_{11} \\ k_{12} \\ \vdots \\ k_{mn} \end{bmatrix}$$

which are vectors of small-angle, three-axis attitude rotation corrections for each time sample l, and a vector of integer biases, respectively, for all combinations of m baselines and n GPS satellites. The right-hand side of the matrix equation is a vector of differential phase residuals, so that the following results:

$$\boldsymbol{\delta\varphi}^{(\ell)}(mn \times 1) = \begin{bmatrix} \delta\varphi_{11}^{(\ell)} \\ \delta\varphi_{12}^{(\ell)} \\ \vdots \\ \delta\varphi_{mn}^{(\ell)} \end{bmatrix}$$

where

$$\delta\varphi_{ij}^{(\ell)} = \Delta\varphi_{ij}^{(\ell)} - \boldsymbol{b}_i^T A_0^{(\ell)} \hat{\boldsymbol{s}}_j^{(\ell)}$$

and $A_0^{(\ell)}$ is the current best estimate of the platform attitude for epoch ℓ.

To this point, it has been assumed that the time scale of platform motion is very much faster than that of the GPS satellites. It is also possible for the time scales of motion for the two to be comparable, such as in space or marine applications. That *quasi static* case can be treated by applying exactly the same nonlinear, least-squares fit equations. The principal difference is that the time interval of measurement collection is increased.

2. *Static Integer Resolution*

In the static case, the solution may also be refined iteratively by linearizing the observation equation. However, because the static platform attitude is the same for all epochs l, the form of linearized observation equation is as follows:

$$\begin{bmatrix} H_1 & \vert & -I \\ H_2 & \vert & -I \\ \vdots & \vert & \vdots \\ H_N & \vert & -I \end{bmatrix} \begin{bmatrix} \delta\theta \\ \hline k \end{bmatrix} = \begin{bmatrix} \delta\varphi^{(1)} \\ \delta\varphi^{(2)} \\ \vdots \\ \delta\varphi^{(N)} \end{bmatrix}$$

Again, the right-hand side is a vector of differential phase residuals. The final solution for the vector k yields the integer ambiguities. For non–co-planar baselines, the estimation process usually has enough information to resolve the ambiguities reliably after about 10 min of satellite motion—even with only two satellites in view.

D. Alternative Means for Cycle Ambiguity Resolution

Although motion-based methods for cycle ambiguity resolution are certainly not the only means for system initialization, they undoubtedly have the highest integrity—especially if no external information is available. There are at least two other "instantaneous" approaches that may also be employed with the potential disadvantage that they require more hardware to implement:

1) *Multiple GPS Antennas:* By using small and large baselines together, it is possible to resolve cycle ambiguities in an explicit sequence by starting with the small baselines (where there is little ambiguity) and working one's way out to the larger baselines. Although the entire process is rapid, additional antennas are required.

2) *Multiple GPS Observables:* Another alternative is to use code ranging to establish the dual-frequency carrier, wide-lane ambiguity, allowing the L_1 cycle ambiguities to be resolved. However, on rare occasions the method may still fail to establish the correct wide-lane ambiguity, and a more expensive dual-frequency receiver is required.

V. Performance

This section examines key aspects of the overall performance of attitude determination using GPS and quantifies the most significant sources of error in attitude determination.

A. Geometrical Dilution of Precision for Attitude

The H matrix from Sec. III is the best means for evaluating the attitude fix accuracy. In general, the attitude error is a function of the satellite geometry, baseline geometry, *and* instantaneous vehicle attitude. Given a differential ranging error of σ (typically 5mm), an estimate of the attitude covariance matrix P is given by $P = (H^T H)^{-1}\sigma^2$, where the 1 σ pointing error (in radians) for any given attitude axis is given by the square root of the corresponding diagonal element of this 3×3 covariance matrix. The diagonal elements correspond to small rotations about the $\boldsymbol{x}'$, $\boldsymbol{y}'$, and $\boldsymbol{z}'$ body frame coordinate axes, respectively.

For generality, the baseline and satellite line-of-sight vectors can be concatenated into matrices B $(3 \times m)$ and S $(3 \times n)$, where $B = [\boldsymbol{b}_1 \quad \boldsymbol{b}_2 \quad \cdots \quad \boldsymbol{b}_m]$ and $S = [\hat{\boldsymbol{s}}_1 \quad \hat{\boldsymbol{s}}_2 \quad \cdots \quad \hat{\boldsymbol{s}}_n]$.

For the ideal baseline configuration where $BB^T = L^2 I$ (where L is the effective baseline length), I is the 3×3 identity matrix, and each of the n GPS satellites is in view of all the antennas on the vehicle, it can be shown that the attitude covariance simplifies to

$$P = [nI - ASS^T A^T]^{-1}\left(\frac{\sigma}{L}\right)^2$$

This form suggests a convenient means for characterizing the suitability of the constellation geometry for attitude determination. As an analog to GDOP, ADOP, the geometric dilution of precision for attitude, is defined by considering the geometrical component of the covariance matrix. Invoking the invariance of the matrix trace with respect to coordinate rotations, the resulting total angular pointing error σ_θ may be written as follows:

$$\sigma_\theta = (\text{ADOP})\,\frac{\sigma}{L}$$

where

$$\text{ADOP} \equiv \sqrt{\text{trace}[(nI - SS^T)^{-1}]}$$

The quantity ADOP is defined even when there are only two satellites in view, the minimum number required for three-axis attitude determination. Its value is generally around unity or smaller, indicating that the GPS constellation consistently provides a favorable geometry for attitude determination.

Thus, a further approximation for the attitude error can be made by simply neglecting the satellite geometry term (ADOP) and considering it to be near unity, so $\sigma_\theta \cong \sigma/L$.

The remaining issue is determining what to use for the value of σ. Table 1 offers typical numbers for relative positioning. In all but the highest regimes of dynamics, the largest error source is multipath.

B. Multipath

Multipath is without question the largest source of error in attitude determination using GPS. Although the actual error it produces is highly deterministic (i.e., a function of the specific environment, materials, antenna gain pattern,

Table 1 Attitude determination ranging error sources (1σ)

Sources	Range error m
Multipath (differential range error for a given pair)	~5 mm
Structural distortion (flexure, thermal expansion)	Application-specific
Troposphere	Modelable
Carrier-to-noise ratio	<1 mm
Receiver-specific errors (crosstalk, line bias, interchannel bias)	<1 mm
Total rss differential ranging error (1σ), excluding distortion	~5 mm

geometry, and other factors), practical experience suggests the approximate rule of thumb that the differential ranging error between a pair of hemispherical microstrip patch antennas is about 5 mm, 1 σ.

In most cases, the most practical and cost-effective approach to systems engineering is simply to use GPS attitude determination in those applications for which this standard multipath error of 5 mm would be acceptable. In cases where more accuracy is required, a number of techniques have been proposed for improving multipath errors. A partial list of techniques includes multipath calibration or antenna pattern shaping,[11] inertial aiding,[13] and mathematical multipath modeling.[14] However, such performance enhancements also carry a penalty of cost or complexity.

C. Structural Distortion

Structural distortion (caused by thermal or flexural bending) can be an issue in certain applications. In most cases, it can either be neglected, modeled, or estimated. (An example of estimating wing flexure on an airplane is given in Fig. 12.)

D. Troposphere

The troposphere can often be a source of error in attitude determination. The simplified model in Fig. 10 shows ray propagation from the vacuum of space down toward the Earth's surface. Refraction of the GPS ranging signal causes the ray to bend downward as atmospheric density (and index of refraction) increases. The simplified slab model depicted in Fig. 10 treats the atmosphere as a block of uniform density and index of refraction n_2. Using Snell's law of refraction

$$\frac{\sin \theta_2}{\sin \theta_1} = \frac{n_1}{n_2}$$

where n_1 is unity, and n_2 (depending upon the atmospheric and water vapor

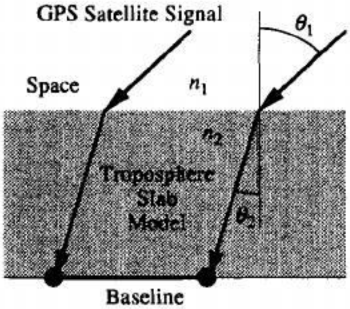

Fig. 10 Atmospheric refraction.

conditions) is somewhere around 1.00026. This simple model can be used to adjust the apparent line-of-sight vectors of the GPS satellites to account for the troposphere in attitude determination applications.

E. Signal-to-Noise Ratio

In applications where it is desirable to track higher dynamics, the tracking loop bandwidth can be opened up (within limitations). The noise on the reconstructed carrier, which dictates the differential range measurement error, is given by the following white noise equation:

$$\sigma = \sqrt{\frac{f_N}{C/N_0}}\frac{\lambda}{2\pi}$$

where f_N is the noise bandwidth of the carrier tracking loop, and C/N_0 is the carrier to noise ratio.[15] Typically, this error is dominated by multipath and is smaller than a millimeter for typical tracking parameters (C/N_0 = 40 dB-Hz, f_N = 10 Hz).

F. Receiver-Specific Errors

Receiver-specific errors, including crosstalk, line bias, and interchannel bias, can be significant sources of error if they are not treated appropriately in a receiver design. Crosstalk between the radio frequency paths for each antenna is an issue, because there is often more than 100 dB of gain along each signal path. Line bias is the nearly constant offset in phase from one antenna to another. A function of both cable length and temperature, line bias is all that remains of the relative clock offset in the design of the common local oscillator. Finally, interchannel bias results from using different hardware channels to measure the carrier phase for each satellite. State-of-the-art receivers employ special techniques to render the errors from all of these effects much smaller than those from multipath.

G. Total Error

Because multipath usually dominates all other error sources (in the absence of significant structural distortion), an approximate and general rule of thumb for attitude determination angular accuracy (in radians) for a representative baseline length of L (in cm) is simply as follows:

$$\boxed{\sigma_\theta \text{ (in radians)} \cong \frac{0.5 \text{ cm}}{L \text{ (in cm)}}}$$

VI. Applications

The capability to use GPS for attitude determination opens up a new realm of applications and opportunities. In the future, it is very likely that the integration of attitude determination into larger systems—including those that use carrier phase for positioning as well—will play a key role in realizing the full potential of GPS. Applications in aviation, spacecraft, and marine areas are summarized below.

A. Aviation

In aviation, heading and attitude sensing using GPS provides a readout that is completely immune to drift and magnetic variation. Many researchers have carried out aircraft experiments to test attitude determination using GPS.[16–19] Figure 11 shows the agreement in roll attitude between GPS and an inertial navigation unit (INU) at a 10-Hz output rate. This flight experiment employed the GPS attitude system that was developed by Stanford University and built

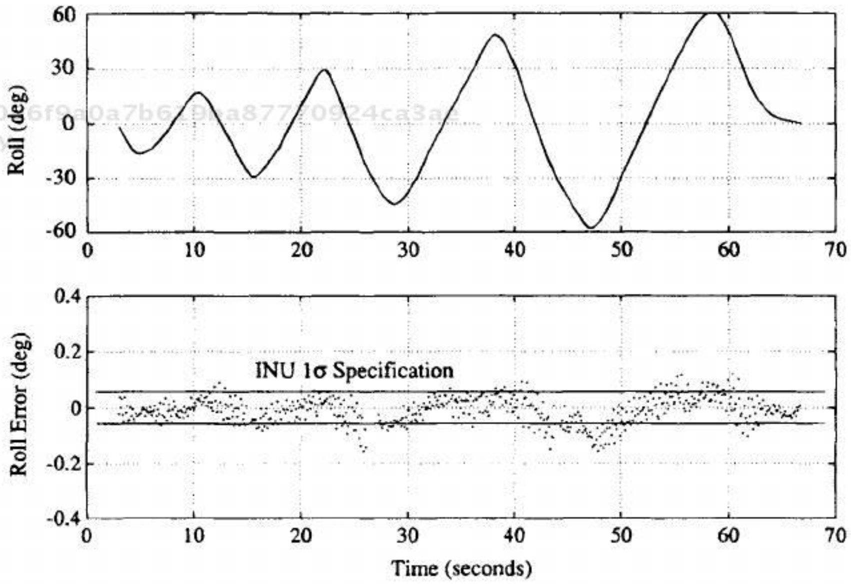

Fig. 11 King Air roll reversals and the inertial navigation unit–GPS agreement.

around a Trimble TANS Quadrex receiver. The system was flown on a NASA Ames King Air, carrying an INU specified to a one sigma accuracy of 0.05 deg. The antennas were mounted on the fuselage, wing tips, and tail, giving the roll component a 16-m baseline. As the aircraft performs roll reversals up to a 60-deg angle of bank, the disparity between roll attitude measured by the two independent sensors seldom exceeds the INU specification. At the steepest angles of bank, the airframe is blocking many of the satellites in view. Sometimes tracking as few as two GPS satellites, the system flawlessly hands off the integers in real time. *In a time span of just a few seconds, the system is tracking a completely new set of satellites with a completely new set of integers.*

A new application of GPS attitude determination is identification of the aircraft dynamic model. The pilot can supply inputs to the controls that excite a dynamic response. The GPS sensor then measures this response to reconstruct an accurate model of the aircraft dynamics. The model then serves as the foundation for optimal autopilot synthesis. Figure 12 shows an example of the characteristic pitch response of an aircraft to a stick input.[12] The "phugoid" response of the aircraft reveals the natural frequency and damping of this mode. It is possible that such model estimation can be carried out continuously in flight, providing a new set of constraints to the position fixes performed by the navigation equipment and, thus, a means for additional integrity checking.

Figure 12 also shows how instantaneous wing flexure is measured to a precision of 1.4-mm rms. The error was evaluated with respect to a best-fit second-order response. Using the same GPS attitude determination system and the antenna arrangement shown in Fig. 5, the structural deformation of the airframe can be used as an indirect means of measuring vertical acceleration.

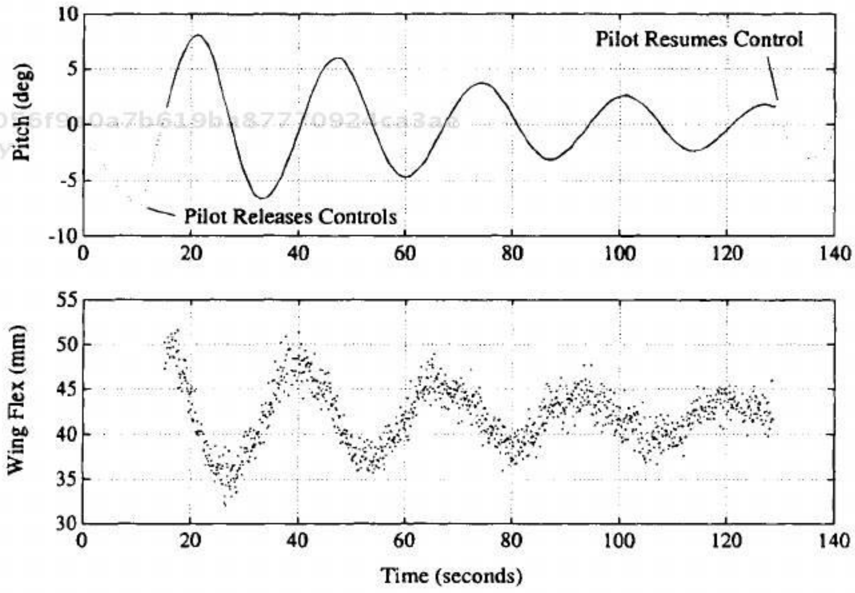

Fig. 12 Piper Dakota phugoid mode state estimates.

By integrating attitude with the enroute navigation, precision landing, collision avoidance, automatic dependent surveillance functions, *a single GPS sensor has the potential to perform the functions of a significant fraction of cockpit instruments currently in use.*

B. Spacecraft

The state-of-the-art in attitude receivers is small (1300 cc), light (~1.5 kg), and low power (~3.5 W), so that one can be carried on just about any spacecraft. Initial experiments with attitude determination on spacecraft[20] indicate that for many types of missions, the GPS may offer significant cost savings. See Chapter 16, this volume, for more information on closed-loop space applications.

C. Marine

In the marine area, the standard for comparison is the gyrocompass. The GPS offers low-cost heading indicator output with rapid start-up times and all-latitude operation. Some of the marine work in attitude determination is described in Refs. 3 and 21.

Attitude determination also provides the potential to point antennas or other directional devices (such as weaponry) on ship-based or other moving platforms. Applying closed-loop control stabilizes the platform against changes in the vehicle orientation.

This partial list of applications hardly begins to address the ultimate potential of attitude determination using the GPS. Given trends in lowering cost, size, weight, and power of GPS technology, it is not inconceivable that backpackers could carry a hand-held portable direction finder that complements the GPS positioning capability. With attitude capability in such a small package, many more applications will undoubtedly arise.

References

[1]Albertine, J. R., "An Azimuth Determination System Utilizing the Navy Navigation Satellites," *Navigation* Vol. 21, No. 1, 1974.

[2]Joseph, K. M., and Deem, P. S., "Precision Orientation: A New GPS Application," International Telemetering Conference, San Diego, CA, Oct., 1983.

[3]Kruczynski, L. R., Li, P. C., Evans, A. G., and Hermann, B. R., "Using GPS to Determine Vehicle Attitude: U.S.S. Yorktown Test Results," *Proceedings of ION GPS-89* (Colorado Springs, CO), Institute of Navigation, Washington, DC, Sept. 1989.

[4]Brown, R., and Ward, P., "A GPS Receiver with Built-in Precision Pointing Capability," *Proceedings, IEEE PLANS, 90, IEEE Position, Location, and Navigation Symposium,* (Las Vegas, NV), Institute of Electrical and Electronics Engineers, New York, March 1990, pp. 83–93.

[5]Kuhl, M., Qin, X., and Cotrell, W., "Design Considerations and Operational Results of an Attitude Determination Unit," *Proceedings of ION GPS-94* (Salt Lake City, UT), Institute of Navigation, Washington, DC, Sept. 20–24, 1994.

[6]Wertz, J. R. (ed.), *Spacecraft Attitude Determination and Control,* Reidel, Boston, MA, 1985.

[7]Cohen, C. E., Cobb, H. S., and Parkinson, B. W., "Two Studies of High Performance Attitude Determination Using GPS: Generalizing Wahba's Problem for High Output Rates and Evaluation of Static Accuracy Using a Theodolite," *Proceedings of ION GPS-92* (Albuquerque, NM), Institute of Navigation, Washington, DC, Sept. 16–18, 1992.

[8]Hatch, R., "Instantaneous Ambiguity Resolution," KIS Symposium 1990, Banff, Canada, Sept. 1990.

[9]Knight, D., "A New Method of Instantaneous Ambiguity Resolution," *Proceedings of ION GPS-94* (Salt Lake City, UT), Institute of Navigation, Washington, DC, Sept. 20–24, 1994.

[10]Brown, R. A., "Instantaneous GPS Attitude Determination," *IEEE Aerospace and Electronics Magazine,* June 1992, p. 3.

[11]Cohen, C. E., "Attitude Determination Using GPS," Ph.D. Dissertation, Stanford Univ., Stanford, CA, Dec. 1992.

[12]Cohen, C. E., and Parkinson, B. W., "Aircraft Applications of GPS-Based Attitude Determination: Test Flights on a Piper Dakota," *Proceedings of ION GPS-92* (Albuquerque, NM), Institute of Navigation, Washington, DC, Sept. 16–18, 1992.

[13]Braasch, M., and van Graas, F., "Guidance Accuracy Considerations for Real-Time Interferometric Attitude Determination," *Proceedings of ION GPS-91* (Albuquerque, NM), Institute of Navigation, Washington, DC, Sept. 1991.

[14]Axelrad, P., Comp, C., and MacDoran, P., "Use of Signal-to-Noise Ratio for Multipath Error Correction in GPS Differential Phase Measurements: Methodology and Experimental Results," *Proceedings of ION GPS-94,* (Salt Lake City, UT), Institute of Navigation, Washington, DC, Sept. 20–24, 1994.

[15]Rath, J., and Ward, P., "Attitude Estimation using GPS," National Technical Meeting ION, San Mateo, CA, Jan. 1989.

[16]Purcell, G. H., Jr., Srinivasan, J. M., Young, L. E., DiNardo, S. J., Hushbeck, E. L., Jr., Meehan, T. K., Munson, T. N., and Yunck, T. P., "Measurement of Aircraft Position, Velocity and Attitude using Rogue GPS Receivers," Fifth International Geodetic Symposium on Satellite Positioning, Las Cruces, NM, March 1989.

[17]van Graas, F., and Braasch, M., "GPS Interferometric Attitude and Heading Determination: Initial Flight Test Results," *Navigation,* Vol. 38, Fall 1991, pp. 297–316.

[18]Cohen, C. E., McNally, B. D., and Parkinson, B. W., "Flight Tests of Attitude Determination Using GPS Compared Against an Inertial Navigation Unit," *Navigation,* Vol. 41, No. 1, 1994.

[19]Cannon, M. E., Sun, H., Owen, T. E., and Meindl, M. A., "Assessment of a Non-Dedicated GPS Receiver System for Precise Airborne Attitude Determination," *Proceedings of ION GPS-94* (Salt Lake City, UT), Institute of Navigation, Washington, DC, Sept. 20–24, 1994.

[20]Cohen, C. E., Lightsey, E. G., Feess, W. A., Parkinson, B. W., "Space Flight Tests of Attitude Determination Using GPS," *International Journal of Satellite Communications,* Vol. 12, Sept.–Oct. 1994, pp. 427–433.

[21]Lu, G., Cannon, M. E., Lachapelle, G., and Kielland, P., "Attitude Determination in a Survey Launch Using Multi-Antenna GPS Technologies," ION National Technical Meeting, San Francisco, CA, Jan. 1993.